

Power Recycling in the Garching 30 m prototype interferometer for gravitational-wave detection

D. Schnier¹, J. Mizuno, G. Heinzel, H. Lück, A. Rüdiger, R. Schilling, M. Schrempel, W. Winkler, and K. Danzmann²

*Max-Planck-Institut für Quantenoptik, Hans-Kopfermann-Str. 1,
D-85748 Garching, Germany, Fax: +49 (89) 32905-200*

Experimental realization of power recycling in an interferometer with 30 m arm-length and suspended optical components has been achieved. The power-recycling factor was about 300, corresponding to a light power of more than 100 W impinging on the beamsplitter. A new concept was used to acquire simultaneous lock of the power-recycling cavity to resonance and of the Michelson phase difference to a dark fringe.

Key words: Power recycling, shot noise, Michelson interferometer, gravitational-wave detector

PACS: 04.80.Nn, 07.60.Ly, 42.25.Hz, 95.55.Ym

1 Introduction

1.1 Historical note

The necessity for high light power in order to reduce the effect of shot noise in the photo-current has been recognized early in the history of interferometric gravitational-wave detectors [1,2]. The idea of enhancing the light power by what has become known as *power recycling* has been proposed at the NATO Advanced Science Workshop in Bad Windsheim (1981), Drever [3] seeing its great potential with modern high-quality mirrors, Schilling pointing out how his 'second frequency control loop' [4] lends itself to the implementation of this scheme for enhancing light power.

¹ e-mail: drs@mpq.mpg.de

² also at: Universität Hannover, Appelstr. 2, D-30167 Hannover

Power recycling, already in its experimentally more demanding implementation with separately suspended masses, but still with short (30 cm) arms, was first reported by Maischberger [5] with moderate recycling factors. Higher recycling factors, albeit in a rigid table-top set-up, were later reported by Man et al. [6]. A significant step forward, in arm-length, in recycling factor, and in the enhanced light power, will be reported in this paper.

1.2 Shot noise in a Michelson interferometer

Michelson interferometers are used for extremely sensitive length measurements as required in, e.g., gravitational-wave detectors. One of the limiting noise sources is the shot noise related to the photo-current in the photo-diode (PD in Fig. 1) at the detection port [7]. In an ideal Michelson interferometer, the (single-sided) power spectral density $S_{\delta L}(f)$ of the fluctuations in path-difference, as simulated by the shot noise, is given by

$$S_{\delta L}(f) = \frac{\hbar c}{\pi} \frac{\lambda}{\eta P_{BS}} \approx (10^{-17} \text{ m}/\sqrt{\text{Hz}})^2 \times \left[\frac{\lambda}{1 \mu\text{m}} \right] \left[\frac{\eta P}{100 \text{ W}} \right]^{-1}, \quad (1)$$

with λ the wavelength of the light, P_{BS} the light power impinging on the beamsplitter, and η the quantum efficiency of the photo-detector. For a given wavelength λ , the shot noise level can be improved by increasing the light power P_{BS} .

However, only a few watts of light power P_0 are available today from well-stabilized lasers that have reasonable values of $\lambda/\eta P_0$. Therefore all interferometric gravitational-wave detectors currently planned or under construction [8–11] include the concept of power recycling [3] as a means of enhancing the effective light power in the Michelson. The basic idea is outlined in the next section.

1.3 The principle of power recycling

The Michelson interferometer³ MI (Fig. 1) is operated at a dark fringe, i.e. the phase difference between the beams returning from the two arms (in the following called the MI-phase) is controlled for destructive interference at the detection port (PD). The light leaving the other port, directed towards the laser, therefore shows constructive interference. As seen from the laser, the interferometer behaves like a mirror with variable reflectivity and transmittance (thus we refer to the light leaving the detecting port as the *transmitted* light).

³ In this paper, the word ‘interferometer’ is used to mean the whole optical system, whereas ‘Michelson interferometer’ (also MI or ‘Michelson’ for short) is used for the beamsplitter and the two arms, excluding the power-recycling mirror.

The reflectivity of the MI can be quite high if the losses due to a finite fringe contrast (see below) and to non-zero end-mirror transmissions are small.

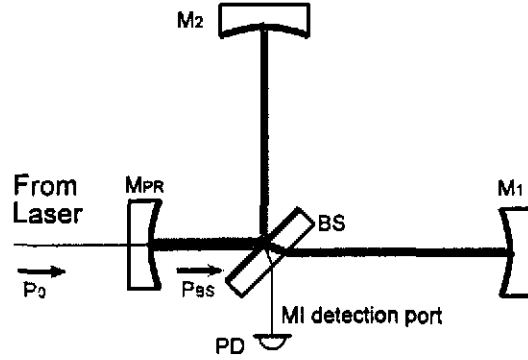


Fig. 1. Michelson interferometer (BS, M_1 , M_2), with power-recycling mirror M_{PR} added.

In order to realize power recycling, an extra mirror M_{PR} (Fig. 1) is inserted between the laser and the beamsplitter BS, thus (together with the MI) forming a cavity (*PR-cavity*) similar to a Fabry-Perot resonator. When this cavity is at resonance, the light power P_{BS} impinging on the beamsplitter is enhanced by the so-called recycling factor G , from the original P_0 to $P_{BS} = GP_0$.

The recycling factor G depends on the amplitude reflectivity ρ_{MI} of the MI and the amplitude transmittance τ_{PR} and reflectivity ρ_{PR} of the PR-mirror,

$$G = \frac{\tau_{PR}^2}{(1 - \rho_{PR}\rho_{MI})^2} \simeq \begin{cases} 4/\tau_{PR}^2 & \text{for } \tau_{PR}^2 \gg 1 - \rho_{MI}^2 \\ 1/\tau_{PR}^2 & \text{for } \tau_{PR}^2 \simeq 1 - \rho_{MI}^2. \end{cases} \quad (2)$$

For given losses $\Lambda = 1 - \rho_{MI}^2$ in an MI, the recycling factor G becomes a maximum when the power transmittance τ_{PR}^2 of the power-recycling mirror equals these losses, the so-called *impedance-matched* case. A cavity with a smaller or larger value of τ_{PR}^2 is called under- or over-coupled, respectively.

1.4 Effect of finite contrast

Realistic mirrors have finite deformations from the ideal shape, and part of the reflected light is scattered into higher order transverse modes [12]. If there is an asymmetry between the deformations of the two end mirrors of an MI, these higher order modes do not necessarily interfere destructively. Thus, a finite fraction of the injected light power leaks out of the MI towards the detection port (similar to an interferometer with different reflectivities in the arms), resulting in a finite (i.e. < 1) fringe contrast. This effect must be included in the losses of the MI.

When operating such an MI with power recycling, the light leaking out of the MI at a dark fringe is also enhanced. If the PR-mirror is chosen to be impedance-matched, the amount of higher-order modes leaking out at a 'dark fringe' can, from conservation of energy, be expected to be as high as that of the injected light power, assuming all losses are due to a finite fringe contrast. Thus the transmitted light power would effectively become a maximum at the 'dark fringe'. In a more realistic case, the MI also has losses which do not contribute to the interference at all (absorption and scattering to very high order modes). Then the transmitted light power can be either a maximum or a minimum at a 'dark fringe', depending on the actual parameters (amount of each kind of loss, reflectivity of PR-mirror).

An example of this behavior is shown in Fig. 2. In this figure, the transmittance of the PR-mirror is fixed ($\tau_{PR}^2 = 0.5\%$) and the dependence on the amount of loss due to finite fringe contrast is considered (other losses are assumed to be zero). When there is no loss, the transmitted light power at the dark fringe is zero, as expected. When the loss is smaller than the power transmittance of the PR-mirror, the transmitted power is still a (local) minimum, but less pronounced. It changes to a maximum when the PR-cavity changes from over-coupled to under-coupled, i.e. when the MI-losses exceed the transmittance of the PR-mirror.

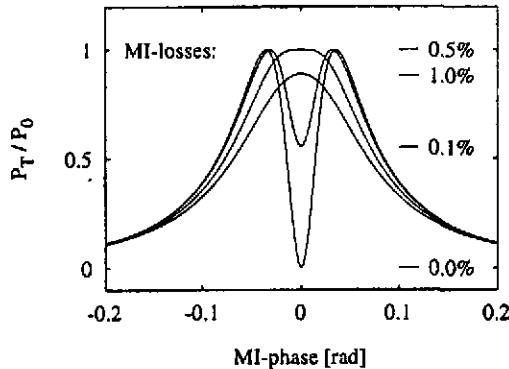


Fig. 2. Calculated light power P_T at the detection port of a power recycled Michelson, as a function of the MI-phase. (The PR-cavity is assumed to be kept on resonance.) Assumptions are $\tau_{PR}^2 = 0.5\%$ and different values of MI-losses Λ due to an anti-symmetric end-mirror deformation.

2 Experimental realization of power recycling

2.1 Experimental set-up

Power recycling has been realized in the Garching 30 m prototype⁴ with suspended optical components, schematically shown in Fig. 3. The light source is an argon ion laser (at $\lambda = 514\text{ nm}$), providing up to 1 W light power in single mode operation. After being transmitted through two Pockels cells PC_1 and PC_2 (which are used for PR-cavity locking, see Section 2.2) and a Faraday optical isolator FR_1 , the light is injected into the interferometer (housed in a vacuum chamber) through a single-mode optical fiber. The light power available after the fiber is $\sim 350\text{ mW}$.

All optical components of the interferometer, including the beam injection unit BI (at the end of the fiber), are suspended as pendulums of approximately 1 m length. The beamsplitter BS is suspended as a double pendulum, all other components as single pendulums. The BI carries the fiber end, a mode matching lens with 15 mm focal length, and a second Faraday isolator FR_2 that directs the light reflected by the PR-cavity to a photo-detector PD_3 .

Two different PR-mirrors M_{PR} were used, both are flat but have different power transmittances τ_{PR}^2 of 7% and 0.54%. The flat fused silica beamsplitter BS, at a distance of 0.5 m behind the PR-mirror, has a measured power transmittance of $\tau_{BS}^2 = 54\%$ at the front coating. The AR-coating on the other surface has a power reflectivity of 300 ppm and thus reflects a small fraction of the light, proportional to the light power P_{BS} impinging on the BS, towards a photo-detector PD_2 .

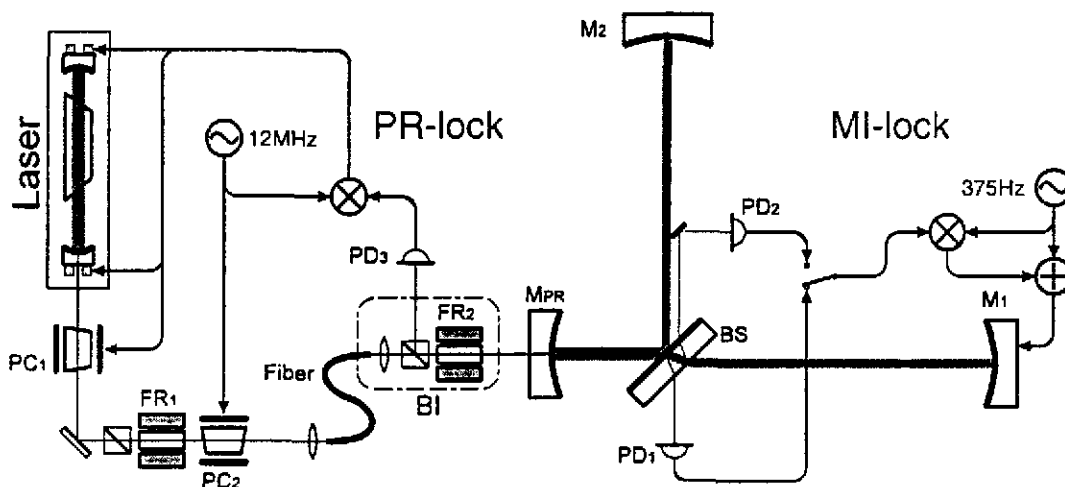


Fig. 3. Experimental set-up.

⁴ The experimental results given in this paper were first presented in January 1996 [13].

The two end mirrors (M_1, M_2) are concave with a curvature radius of 33 m, and are placed 31 m away from the PR-mirror. Both mirrors are highly reflective but show small astigmatism that are rather similar to each other (probably due to the coating process). The major axes of this astigmatism of the two end mirrors happened to be nearly orthogonal while the experiments described here were carried out, i.e. the deformation was almost purely anti-symmetric between the two arms. Therefore the deformation did not significantly change the beam parameters of the cavity eigenmode but led to scattering into higher-order transverse modes, here mainly second order modes [12].

These higher-order modes will leak out of the MI towards the detection port, even if the MI is set to a 'dark fringe'. From the observed fringe contrast of 0.994 with optimum alignment of mirror orientations (but excluding rotation of the astigmatism axes; see below), the losses of the MI due to end-mirror deformation are calculated as $\Lambda = 0.3\%$.

In our set-up, the astigmatism of each end mirror generated a TEM_{11} mode whose nodal lines are rotated by 45° from the astigmatism axes. Due to the fact that we accidentally oriented the two end mirrors in such a way that the axes of their respective astigmatism are almost orthogonal to each other, the TEM_{11} modes from the two arms interfere constructively at the output port of the interferometer. (At the time when the experiment was carried out, we did not recognize the astigmatism of the mirrors and thus did not optimize the astigmatism axes.)

2.2 Preliminary experiments

As preliminary experiments, we first investigated the locking of the MI (without PR-mirror) and that of a 30 m-cavity (without MI), independently, in order to develop a proper control technique for each degree of freedom. The MI without power recycling could be realized either by removing or by intentionally misaligning the PR-mirror so that it did not compose a cavity. On the other hand, the 30 m-cavity without MI is composed of the PR-mirror and the end mirror M_1 , realized by removing the BS. This 30 m-cavity is similar to the PR-cavity when the MI is at a dark fringe.

The MI was locked to a dark fringe by applying a small, low-frequency (375 Hz) modulation to the position of M_1 via a coil-and-magnet arrangement. The transmitted power detected by PD_1 was synchronously demodulated at this frequency. If the MI-phase has only a small offset from a dark fringe, the error signal obtained is proportional to the MI-phase offset, to the modulation index, and to the light power impinging on the MI.

The 30 m-cavity was kept resonant with the laser frequency by using the Pound-Drever technique [14]. There are two (almost) equivalent ways to realize

this: either tuning the laser frequency or controlling the cavity length. In our experimental set-up, the laser frequency was tuned by using two PZTs (fast and slow) attached to the laser-cavity mirrors and by the Pockels cell PC_1 placed outside the laser. The incoming laser beam is phase modulated at 12 MHz by PC_2 , and the error signal is obtained by synchronously demodulating the reflected light (detected by PD_3) at that modulation frequency.

2.3 First step of acquiring lock

For a power recycled Michelson interferometer, the two parameters described in the previous section (the MI-phase and the tuning of the laser frequency) must be controlled *simultaneously*. The power recycling factor $G = P_{BS}/P_0$ reaches its maximum when the laser frequency is resonant with the PR-cavity *and* the MI-phase is at a dark fringe. Acquiring lock of both parameters is complicated because each parameter affects the characteristics of the other control. Either parameter can in principle be controlled first, but with a different consequence for the experimental realization.

When one tries to lock the MI to a dark fringe with the PR-mirror in place, one faces the problem of vastly fluctuating light power as caused by the uncontrolled motions of the PR-cavity between resonance and anti-resonance. Correspondingly the gain for the MI-locking signal, being proportional to P_{BS} , fluctuates by many orders of magnitude. This causes severe problems with the stability of the servo loops, even though it can in principle be compensated by a sufficiently fast automatic gain control.

In practice, another approach turned out to be more promising: the laser frequency can be locked to resonance of the PR-cavity independent of the MI-phase. This PR-cavity is equivalent to a Fabry-Perot cavity with fluctuating transmittance of the rear mirror. The DC gain of the Pound-Drever technique is roughly proportional to the cavity finesse which in this case depends on the MI-phase. When the MI-phase is at a bright fringe, the Pound-Drever signal becomes a minimum. For a symmetric beamsplitter and equal losses in the two arms, the signal will be zero at this point (because no light is reflected from the MI), and thus the PR-cavity loop would become unstable.

Here the initially unintended asymmetry of our BS ($\tau_{BS}^2 = 54\%$) turned out to be helpful: the MI always reflects some light, even when the MI-phase is at a bright fringe, and thus the Pound-Drever technique always generates an error signal. In our experiment the DC gain of the loop fluctuates by a factor of order 10^4 , but continuous lock of the laser frequency was possible even when the MI-phase changes by more than π (see left part of Figs. 4 and 5). This 'robustness' of the loop is partly due to the fact that the cavity bandwidth (and thus the capture range) is broad when the gain is low, and also due to

the ‘unconditionally’ stable design of our control loop for the laser frequency.

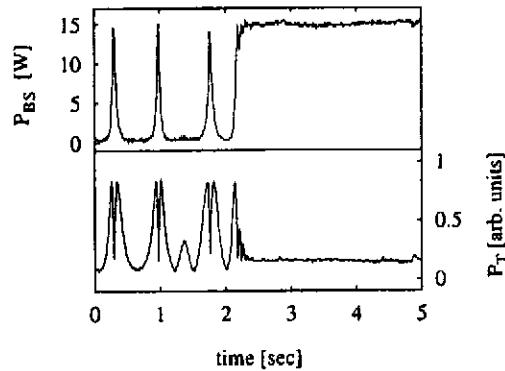


Fig. 4. The measured transmitted and internal powers, P_T and P_{BS} , with the 7% PR-mirror during the second step of acquiring lock. The fluctuating MI-phase is locked to the dark fringe at $t = 2.1$ sec.

2.4 Second step of acquiring lock

After locking the PR-cavity that contains the fluctuating MI, the MI-phase must be locked to a dark fringe. With the PR-mirror of $\tau_{PR}^2 = 7\%$ installed, it was possible to use the same scheme as for the MI without power recycling. The gain of the loop was, however, reduced in order to compensate for the increased error signal due to the enhanced light power.

Because the locking range of the MI-lock is confined between the two maxima of the transmitted power (see Fig. 2), the MI-phase was not immediately locked when the servo loop was closed. Locking is achieved only when the MI-phase is inside the locking range and when the random motion of the optical components are not too fast. It was possible to reduce the acquisition time by using an ‘intermediate’ step, that is to lock the MI-phase to one of the maxima of transmitted power in Fig. 2. This was achieved by inverting the polarity of the MI-locking signal. At this intermediate state, the MI-phase is already close to the desired dark fringe which can finally be reached by switching the MI-locking signal back to the original polarity.

After acquiring both locks, stable operation of the cavity with a nearly constant PR factor was possible for more than an hour without any readjustment. The recycling factor G was measured by comparing the internal power GP_0 during PR operation with $\tau_{PR}^2 P_0$, obtained by misaligning the PR-mirror in order to make PR inactive. The result $G \approx 50$ was in good agreement with $G \approx 51$ calculated with $\tau_{PR}^2 = 7\%$ and $\Lambda = 0.3\%$.

With the more highly reflective PR-mirror of $\tau_{PR}^2 = 0.54\%$ installed, it turned out that the standard MI-locking scheme, as described in Section 2.2, could

no longer be used. Because the losses in the MI are now comparable with τ_{PR}^2 and are dominated by mirror deformation, the small low-frequency modulation failed to find the 'dark fringe'. This is because the minimum at the dark fringe became less pronounced (see Fig. 2).

In addition, there is a strong asymmetry between the two maxima of the transmitted power (see Fig. 5; e.g. the resonance with two peaks at 0.51 sec) which disturbs the MI-locking loop. We suspect that the higher-order modes generated by scattering at the end mirrors cause an offset in the Pound-Drever signal, depending on the MI-phase, when the interferometer is close to the dark fringe. Another cause of the asymmetry is the finite aperture in the optical path before PD_1 , which truncates some of the higher order modes.

In order to overcome this problem, we used the internal power detected at PD_2 (instead of the transmitted power detected at PD_1) to generate the error signal for the MI-phase control. This error signal (with inverted polarity) is fed back to the MI so that the *internal* power is maximized.

As expected, much higher values for the recycling factor were obtained with the more highly reflective PR-mirror. The PR factor was $G \approx 300$, again measured by comparing the internal power with and without PR. The result is in good agreement with the value of $G \approx 306$ expected theoretically for the given transmittance τ_{PR}^2 of the PR-mirror and the losses Λ of the MI. However, the long term stability of the system was reduced. Stable operation with both locks working was possible for about 15 minutes before drifts in the alignment of the optical components necessitated readjustment. The recycling factor G dropped during this period by a factor of ~ 2 . Periodic variations observed in the transmitted and internal power during the operation (see right hand side of Fig. 5) can be related to eigenfrequencies of the tilt modes of the suspended optical components. These alignment problems will be overcome when the auto-alignment system currently being developed is implemented.

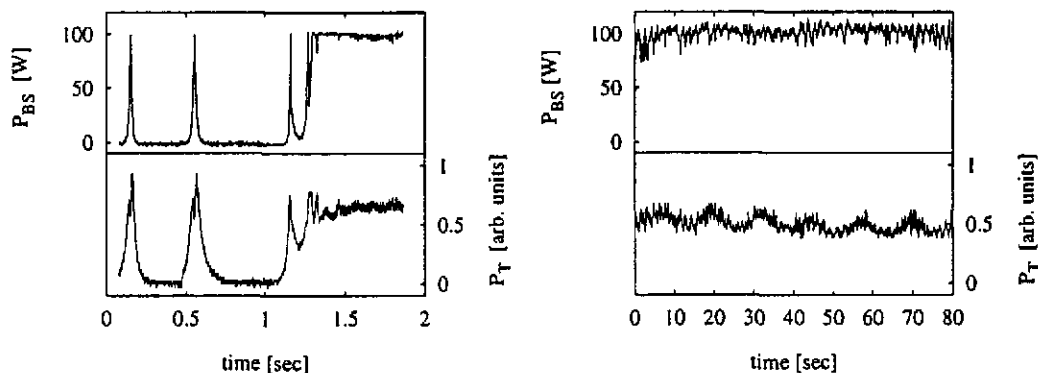


Fig. 5. The measured transmitted and internal powers, P_{T} and P_{BS} , with the 0.54% PR-mirror during the second step of acquiring lock (left) and during the operation of power recycling (right, with a compressed time scale.)